

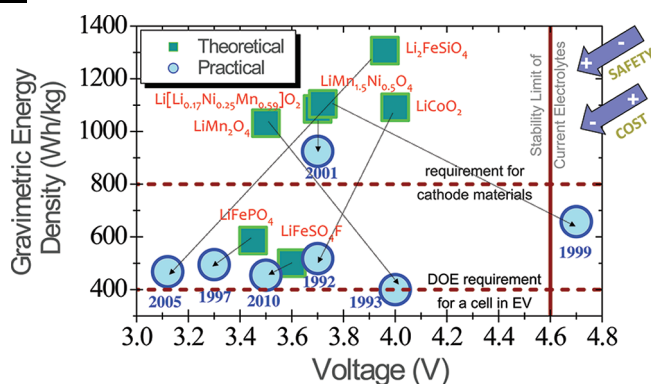
# Recent Advances in First Principles Computational Research of Cathode Materials for Lithium-Ion Batteries

YING SHIRLEY MENG<sup>\*,†</sup> AND M. ELENA ARROYO-DE DOMPABLO<sup>\*,‡</sup>

<sup>†</sup>Department of NanoEngineering, University of California San Diego, La Jolla, California 92109, United States, and <sup>‡</sup>MALTA-Consolider Team, Departamento de Química Inorgánica, Facultad de Ciencias Químicas, Universidad Complutense de Madrid, Madrid 28040, Spain

RECEIVED ON SEPTEMBER 14, 2011

## CONSPECTUS



To meet the increasing demands of energy storage, particularly for transportation applications such as plug-in hybrid electric vehicles, researchers will need to develop improved lithium-ion battery electrode materials that exhibit high energy density, high power, better safety, and longer cycle life. The acceleration of materials discovery, synthesis, and optimization will benefit from the combination of both experimental and computational methods. First principles (*ab Initio*) computational methods have been widely used in materials science and can play an important role in accelerating the development and optimization of new energy storage materials. These methods can prescreen previously unknown compounds and can explain complex phenomena observed with these compounds.

Intercalation compounds, where Li<sup>+</sup> ions insert into the host structure without causing significant rearrangement of the original structure, have served as the workhorse for lithium ion rechargeable battery electrodes. Intercalation compounds will also facilitate the development of new battery chemistries such as sodium-ion batteries. During the electrochemical discharge reaction process, the intercalating species travel from the negative to the positive electrode, driving the transition metal ion in the positive electrode to a lower oxidation state, which delivers useful current. Many materials properties change as a function of the intercalating species concentrations (at different state of charge). Therefore, researchers will need to understand and control these dynamic changes to optimize the electrochemical performance of the cell. In this Account, we focus on first-principles computational investigations toward understanding, controlling, and improving the intrinsic properties of five well known high energy density Li intercalation electrode materials: layered oxides (LiMO<sub>2</sub>), spinel oxides (LiM<sub>2</sub>O<sub>4</sub>), olivine phosphates (LiMPO<sub>4</sub>), silicates-Li<sub>2</sub>MSiO<sub>4</sub>, and the tavorite-LiM(XO<sub>4</sub>)F (M = 3d transition metal elements). For these five classes of materials, we describe the crystal structures, the redox potentials, the ion mobilities, the possible phase transformation mechanisms, and structural stability changes, and the relevance of these properties to the development of high-energy, high-power, low-cost electrochemical systems. These results demonstrate the importance of computational tools in real-world materials development, to optimize or minimize experimental synthesis and testing, and to predict a material's performance under diverse conditions.

## 1. Introduction

The performance of today's *energy storage materials* falls short of requirements for using electrical energy efficiently in transportation, commercial, and residential applications,

where the performance requirements significantly differ from those for portable electronic devices. Lithium ion batteries (LIB) offer higher energy density and a longer cycle life than other battery technologies, and have been used as

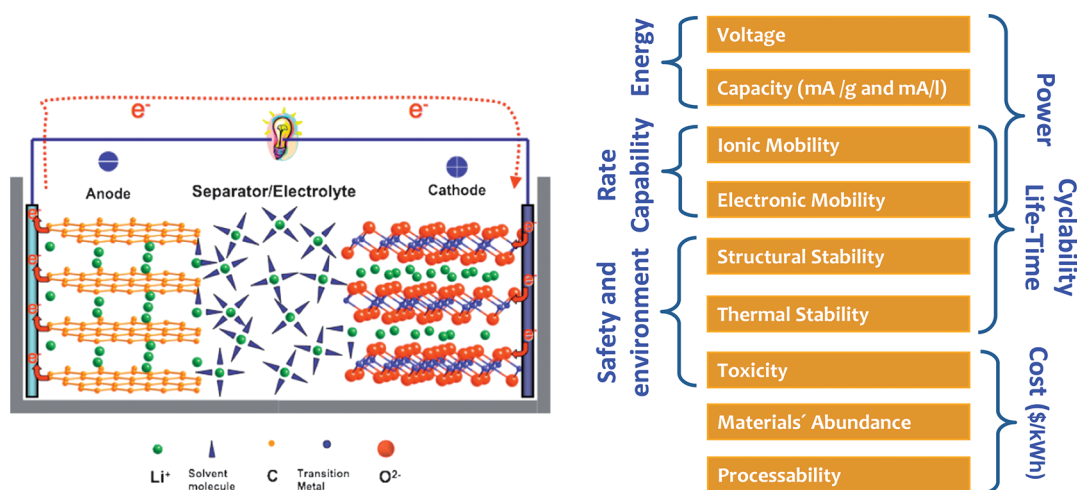


**FIGURE 1.** Schematics of a lithium ion electrochemical cell and the relevant parameters of Li battery electrode materials in relation to battery characteristics.

a key component of portable electronic devices. They may offer a possible near-term solution for environmentally friendly transportation and grid-stability regulation for renewable energies sources such as solar- and wind-power. To meet the increasing energy and power demand, particularly in terms of \$/kWh and/or \$/kW while keeping safety characteristics in check, advances in new materials for LIB are urgently needed.

Many interrelated chemical and physical processes occur in electrochemical energy storage materials under the operating conditions of a rechargeable battery. Electrical energy is generated by conversion of chemical energy via redox reactions. Multiple processes happen at different time and length scales, including charge transfer (micro- to milliseconds) and mass transport (seconds to hours) within the bulk of the materials, as well as across the electrode and electrolyte interfaces; moreover, structural changes and phase transitions (seconds, hours to days) can happen according to the state of the charge. These dynamic processes determine the main parameters of an energy storage system: energy density, charge–discharge rate (power density), cycle lifetime, and safety. The simple schematic in Figure 1 reveals the fact that the electrode materials function as “living” systems within which electrons and ions are moving during charge and discharge. These electronic and ionic motions often trigger structural changes, defect generation, and phase transformations, consequently resulting in significant changes in energy density and rate capability of the entire battery.

First principles (*ab initio*) modeling refers to the use of quantum mechanics to determine structure or property of materials. *Ab initio* computation methods are best known for precise control of structures at the atomic level,

constituting perhaps the most powerful tool to predict structures, and with computational quantum mechanics, many ground state properties can be accurately predicted prior to synthesis. More importantly, the reliability and accuracy of the computational approaches can be significantly improved if experimental information is well integrated to provide realistic models for computation. Experiments and computation are complementary in nature. Many intrinsic properties of electrode materials, including voltages, structure stability, lithium diffusivity, band structure, and electronic hopping barriers can now be computed accurately with first-principles computation methods. Significant inroads have also been made in predicting the thermal stability and surface properties of electrode materials. Over the past decade, we have seen examples where a combination of virtual materials design/characterization and knowledge-guided experimentation have made significant impacts on changing the traditional trial-and-true way of materials design; many of them have accelerated the pace of development of new high energy high power density electrode materials for LIB. A good compendium of such investigations is offered in a previous review article.<sup>1</sup> Recently, high-throughput computational methods have been implemented<sup>2</sup> and utilized to screen for novel electrode materials.<sup>3,4</sup> Based on the predictions from the high throughput work, some new exciting chemistries are currently being explored by the experimentalists worldwide.

Regarding any battery technology, measures of its performance (cell potential, capacity, or energy density and power density) are related to the *intrinsic* properties of the materials that form the positive and negative electrodes

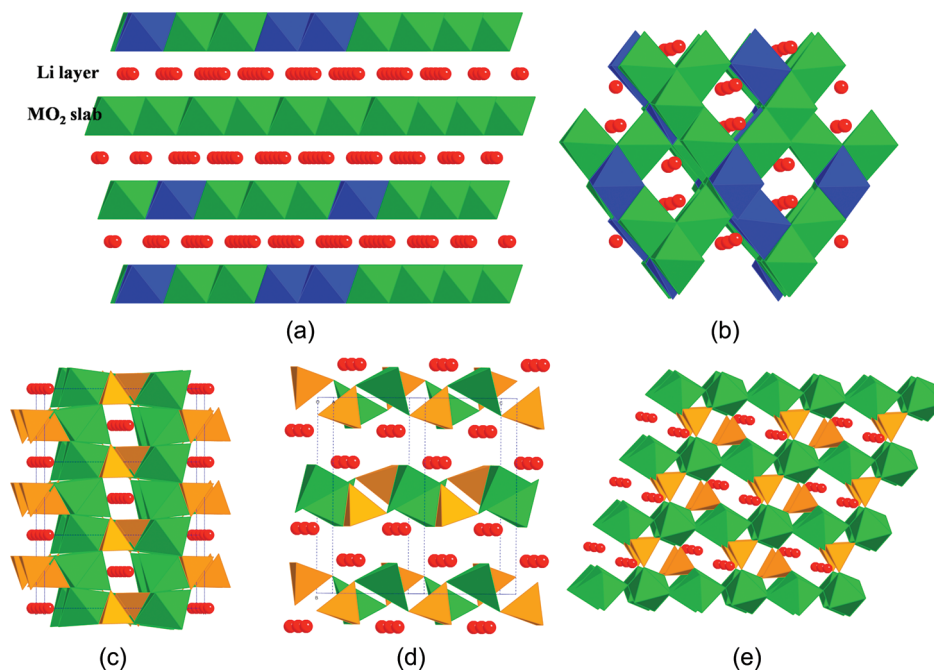


**FIGURE 2.** Crystalline structures of (a) layered-Li[Ni<sub>1/4</sub>Li<sub>1/6</sub>Mn<sub>7/12</sub>]O<sub>2</sub>, (b) spinel-LiM<sub>0.5</sub>Mn<sub>1.5</sub>O<sub>4</sub>, (c) olivine-LiFePO<sub>4</sub>, (d) Li<sub>2</sub>MSiO<sub>4</sub>, and (e) LiFeSO<sub>4</sub>F. TM in green and blue, Li in red, and phosphorus and sulfur in orange.

(Figure 1). The cycle life and shelf life are dependent on the nature of the electrode materials and electrode/electrolyte interfaces, whereas safety is a function of the stability of the electrode materials and electrolytes, as well as the engineering design of the batteries. In this Account, we focus on recent progress made in first-principles computation investigation toward understanding, controlling, and improving the intrinsic properties of high energy density electrode materials in lithium based electrochemical systems.

## 2. Crystal Structure and Electrochemical Characteristics of Relevant Electrode Materials

Currently commercialized positive electrode materials belong to three classes of crystal chemistries: layered oxides (LiMO<sub>2</sub>), spinel oxides (LiM<sub>2</sub>O<sub>4</sub>), and olivine phosphates LiMPO<sub>4</sub> (M = 3d transition metal elements such as Co, Mn, Fe, etc.) Two new classes of promising materials have emerged in the last years, the silicates-Li<sub>2</sub>MSiO<sub>4</sub> and the fluorides-LiM(XO<sub>4</sub>)F. Figure 2 shows the crystal structures of each family.

**2.1. Oxide Electrode Materials.** Layered LiMO<sub>2</sub> crystallize in the α-NaFeO<sub>2</sub> structural type (S.G. *R* $\bar{3}$ *m*) shown in Figure 2a. The structure can be viewed as “ordered rocksalt” in which alternate layers of Li<sup>+</sup> and TM<sup>3+</sup> ions (TM = transition metal oxides) occur in octahedral sites within the cubic close packed oxygen array. The lithium ions can be

reversibly removed from and reinserted between the (MO<sub>6</sub>) layers. A second class of oxide materials (Figure 2b) crystallizes in the spinel structure, S.G. *Fd* $\bar{3}$ *m*, with Li ions in tetrahedral *8a* sites, TM atoms in the octahedral *16d* sites and the oxygen ions occupying the *32e* sites arranged in an almost cubic close-packed manner. The resulting M<sub>2</sub>O<sub>4</sub> framework of edge-sharing octahedra (*16d* and *32e* sites) provides a three-dimensional network of tunnels where the Li ions are located and throughout which these mobile Li ions can diffuse.

**2.2. Polyoxoanionic Electrode Materials.** Figure 2c shows the structure of olivine-LiMPO<sub>4</sub> (S.G. *Pnma*). It can be described as a hexagonal close-packing of oxygen with Li and TM ions located in half of the octahedral sites and P in one-eighth of the tetrahedral positions. The MO<sub>6</sub> octahedra share four corners in the *cb*-plane, being cross-linked along the *a*-axis by the PO<sub>4</sub> groups, whereas Li ions are located in rows, of edge-shared LiO<sub>6</sub> octahedra running along the *b*-axis in between two consecutive [MO<sub>6</sub>] layers. The most frequent crystal structure of Li<sub>2</sub>MSiO<sub>4</sub> (Figure 2d) is related to β-Li<sub>3</sub>PO<sub>4</sub> (S.G. *Pmn*2<sub>1</sub>). It consists of infinite corrugated layers of composition [SiMO<sub>4</sub>]<sub>∞</sub> lying on the *ac*-plane and linked along the *b*-axis by LiO<sub>4</sub> tetrahedra. Within these layers, each SiO<sub>4</sub> tetrahedron shares its four corners with four neighboring MO<sub>4</sub> tetrahedra, and vice versa. Fluorocompounds LiM(XO<sub>4</sub>)F (X = p-block element) crystallize with the structure of the mineral Tavorite (LiFePO<sub>4</sub>(OH)). This

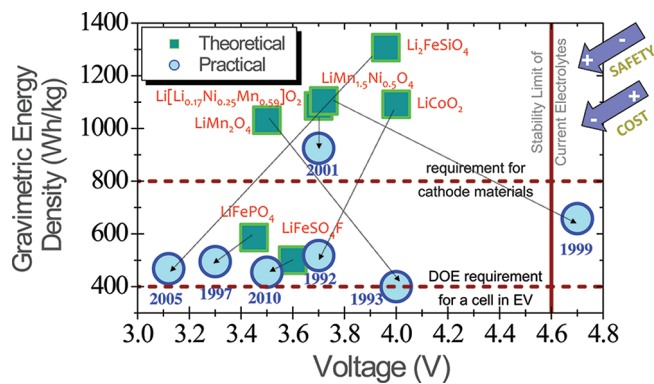


**FIGURE 3.** Overview of gravimetric energy density for different chemistries.

structure comprises a three-dimensional network built up from  $\text{XO}_4$  tetrahedra and  $\text{MO}_4\text{F}_2$  octahedra: the F ions are located in anionic positions not belonging to the phosphate groups (Figure 2e). From  $\text{LiMXO}_4\text{F}$ , it is possible to reversibly deintercalate one Li ion:  $\text{LiFeSO}_4\text{F} \rightarrow \text{FeSO}_4\text{F} + \text{Li}$ . Yet the structure could accommodate a second lithium ion per TM ion, and for certain chemistries it might be possible to reversibly exchange two electron per TM ion.

Figure 3 summarizes the relevant electrode characteristics of the prototype compound of each family. Theoretical specific energies refer to the maximum possible exchange of Li ions per formula unit. In most cases, the crystal structures suffer from certain instability at high degrees of delithiation, and hence, phase transformations, amorphization, dissolution in the electrolyte, or decomposition of the electrode material precludes the practical utilization of the whole theoretical energy. An overly high lithium insertion voltage, not accessible with the current electrolytes, can be an additional constraint to reach the full theoretical capacity. Evidently, energy density requirements for cathode materials depend on the battery applications (stationary, medical and portable devices, etc.). Figure 3 highlights the need for materials improvements to meet the demanded gravimetric energy for electrical vehicle application (EV).

With the final goal of designing a better electrode material, the development of a new class of materials generally takes as starting point the improvement of concrete characteristics of a previous class of materials. As large scale applications of lithium ion batteries are on the horizon, safety issues have become of increasing concern. Phosphate compounds were introduced in the late nineties in the pursuit of an improvement on the safety characteristics of the oxides electrode materials known of at that time. It was the need to increase the specific capacity of oxides and olivine materials that brought the silicates  $\text{Li}_2\text{MSiO}_4$  to the field

in 2005. Favorite-like  $\text{LiMXO}_4\text{F}$  seek for a high lithium intercalation voltage and high lithium mobility without paying a penalty in thermal stability. A progressive improvement of the electrode characteristics has also been achieved within the well-known materials family across the years. Research has been intensive in the layered oxides in the last decades: from the  $\text{LiCoO}_2$  reported in 1980 to the now promising Li excess materials  $\text{Li}[\text{Ni}_x\text{Li}_{1/3-2x/3}\text{Mn}_{2/3-x/3}]\text{O}_2$  ( $0 < x < 1/2$ ). In the next sections, we will show that extensive density functional theory (DFT) investigations have been performed on the aforementioned electrode materials, complementary to experiments, which have led to the improvement of the electrode characteristics.

### 3. Oxide Materials

While initial lithium cells considered sulfur compounds as cathode materials ( $\text{TlS}_2$ ), it was soon realized that transition metal oxides reunited unique properties: high voltage, lightweight, good chemical stability, and good electronic and ionic mobility. As inferred from Figure 3, oxide materials are still the main candidates for high energy density applications.

**3.1. Layered Oxides  $\text{LiMO}_2$ .** For the single metal compounds ( $M = \text{Mn}, \text{Co}, \text{Ni}$ ), early DFT works have shown that different electrochemical characteristics originate from the electronic configuration of the transition metal ion (see ref 5 and references therein). In a layered O3-type structure, lithium diffusion takes place in the lithium layer by hopping from one octahedral site to another octahedral site through an intermediate tetrahedral site. A systematic computational study<sup>6</sup> on factors that influence the activation barrier for Li diffusion in O3 layered oxides led to significant improvements of the high power cathode material  $\text{LiNi}_{1/2}\text{Mn}_{1/2}\text{O}_2$ .<sup>7</sup> Significant computational efforts, combined with experiments, have been devoted to identify the three-dimensional cation ordering in this system and how the ordering changes with the state of charge/discharge.<sup>8</sup>

“Li-excess” layered oxides, formed as a solid solution between  $\text{Li}[\text{Li}_{1/3}\text{Mn}_{2/3}]\text{O}_2$  and  $\text{LiMO}_2$  ( $M = \text{Ni}, \text{Mn}, \text{Co}$ ), are promising candidates for the main on-board storage technology in plug-in hybrid electric vehicles as they offer much higher capacity ( $>250 \text{ mAh/g}$ ).<sup>9</sup> Computational first-principles study of the Li-excess layered oxide compound  $\text{Li}[\text{Ni}_{1/4}\text{Li}_{1/6}\text{Mn}_{7/12}]\text{O}_2$  revealed a new lithium deintercalation mechanism where stable tetrahedral lithium ions are formed during the early charging stage and may not be able to be extracted before 5 V.<sup>10</sup> An atomistic model for a defect spinel-like phase has been proposed for the first time. When partially delithiated, the compound  $\text{Li}_{2/3}\text{Ni}_{1/4}\text{Mn}_{7/12}\text{O}_2$  can be rewritten as  $\text{Li}[\text{Li}_{1/3}\text{Ni}_{1/2}\text{Mn}_{7/6}]\text{O}_4$ , forming a Li-excess

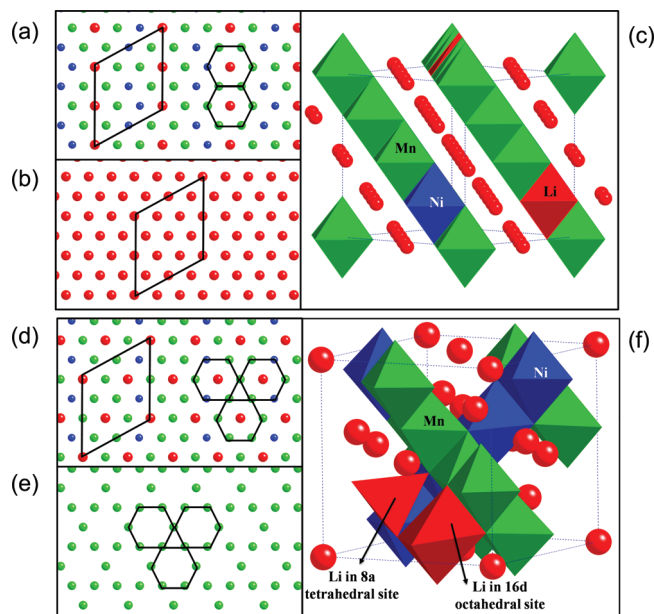


**FIGURE 4.** Crystal structure model of layered  $\text{Li}[\text{Ni}_{1/4}\text{Li}_{1/6}\text{Mn}_{7/12}]\text{O}_2$ : (a) the TM layer; (b) the Li layer, and (c) a particular orientation showing the spinel cubic form. Crystal structure of the defect-spinel model of  $\text{Li}[\text{Ni}_{1/4}\text{Li}_{1/6}\text{Mn}_{7/12}]\text{O}_2$ : the TM layer comparison of (d) defect vs (e) perfect spinel and (f) a particular orientation that reveals the layered form. Taken from ref 10 Reproduced by permission of The Royal Society of Chemistry.

defect-spinel phase where part of the  $16d$  octahedral sites are occupied by Li ions (Figure 4). In a perfect spinel phase, only transition metal ions reside on  $16d$  sites. The proposed phase transformation may partially contribute to the first cycle irreversible capacity and are the main reason for the intrinsically poor rate capability of the Li-excess layered oxide materials.

**3.2. Spinel Oxides.** In  $\text{LiMn}^{3+}\text{Mn}^{4+}\text{O}_4$  besides lithium removal (oxidation of  $\text{Mn}^{3+}$  to  $\text{Mn}^{4+}$  at ca. 4 V), lithium ions can be inserted in the octahedral sites not occupied by Mn leading to  $\text{Li}_2\text{Mn}_2\text{O}_4$  (reduction of  $\text{Mn}^{4+}$  to  $\text{Mn}^{3+}$  at ca. 3 V). Lithium insertion occurs by a two phase mechanism involving a transition from cubic  $\text{Li}[\text{Mn}_2]\text{O}_4$  to tetragonal  $\text{Li}_2[\text{Mn}_2]\text{O}_4$ , which supposes a large  $c/a$  ratio variation of 16% and a unit cell volume variation of 5.6%.<sup>11</sup> This undesirable transformation precludes the utilization of the whole theoretical capacity of  $\text{LiMn}_2\text{O}_4$ . A better understanding of the phase transformation has been recently achieved using DFT+U methods.<sup>12</sup>

The practical specific capacity of  $\text{LiMn}_2\text{O}_4$  arises from the deinsertion of lithium ions and oxidation of  $\text{Mn}^{3+}$  to  $\text{Mn}^{4+}$  at 4 V.  $\text{LiMn}_2\text{O}_4$  tends to exhibit capacity fading in this 4 V region, particularly at elevated temperatures. The partial substitution of Mn by another transition metal is a common alternative to ameliorate this drawback. This strategy has

led to a new family of cation-substituted spinels with the general formula  $\text{LiM}_x\text{Mn}_{2-x}\text{O}_4$ , where  $\text{M} = \text{Ti}, \text{V}, \text{Cr}, \text{Fe}, \text{Ni}, \text{Co}, \text{Cu}$ . In addition to an improvement of the capacity retention on cycling, these spinels have the ability to exhibit an extra capacity above 4.5 V for some transition metal ions. DFT+U methods have been used to screen the first row transition metal ions, demonstrating the effects of codoped element M on the voltage profile and lithium diffusion activation barriers.<sup>13</sup> Careful examination of the electronic structures of the codoped  $\text{LiM}_x\text{Mn}_{2-x}\text{O}_4$  with different TM ions shows that Ti, V prefers to be 4+, pushing part of the Mn to 3+, while Ni, Co, and Cu prefers to be 2+, leaving all the Mn as 4+, which directly affect the voltage characteristics. Figure 5 shows the calculated Li diffusion barriers with different dopants. As compared to the Li diffusion barrier in  $\text{LiMn}_2\text{O}_4$ , the average diffusion barrier increases with Ti, V, and Cr doping and decreases with Co and Cu doping.

Cu is therefore an interesting doping element. However, the electrochemical behavior of Cu-substituted spinels is complex, partly due to the unavoidable oxygen deficiency in the experimentally prepared samples. Joint experimental and DFT+U studies<sup>14,15</sup> of  $[\text{Cu}_{0.5}\text{Mn}_{1.5}]_{\text{Oct}}\text{O}_{4-\delta}$  spinels confirmed that the oxygen deficiency originates from the partial reduction of  $\text{Mn}^{4+}$  to  $\text{Mn}^{3+}$ . An increasing oxygen deficiency results in a greater charge capacity in the low-voltage region (around 4 V) due to the higher  $\text{Mn}^{3+}$  content. For the high voltage region (around 4.8 V, redox couple  $\text{Cu}^{2+}/\text{Cu}^{3+}$ ), it was found that the electrochemical inactivity of tetrahedral Cu rather than the oxygen content is likely the origin of the poor charge capacity observed.

## 4. Polyoxoanionic Materials

Cathode materials consisting of oxygen and transition metals become highly oxidized and susceptible for degradation through exothermic and endothermic phase transitions. The ability of the charged cathode to release oxygen and combust the flammable organic electrolyte ultimately leads to fire. This raised the interest in polyoxoanionic materials, under the view that the strength of the X–O bond would provide a robust framework capable of sustaining large degrees of lithium deintercalation without safety hazards. High throughout ab initio calculations has been recently used to reinvestigate whether phosphate materials are inherently safe.<sup>4</sup> For a large data set of phosphates, the authors found that, for the same metal oxidation state, oxygen release happens thermodynamically at lower temperatures for phosphates than for oxides. This means that the thermal stability of a compound is more driven by the oxidation state

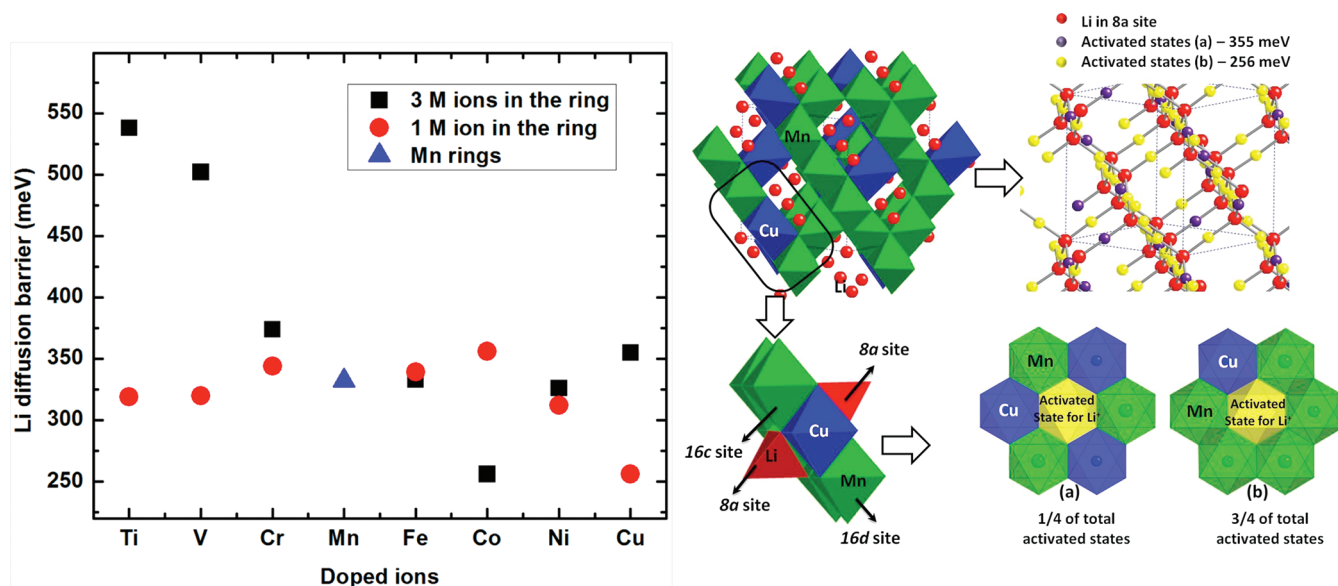


**FIGURE 5.** Li diffusion barriers in  $\text{LiM}_{0.5}\text{Mn}_{1.5}\text{O}_4$  ( $M = \text{Cr}, \text{Fe}, \text{Co}, \text{Ni}, \text{Cu}, \text{Mn}$ ) calculated by GGA and the local environments of transition metal ion rings that lithium ions migrate in the spinel structure. Adapted with permission from 13. Copyright 2011 American Chemical Society.

of the transition metal than by the presence of a P–O bond. The most common oxygen evolution reaction from phosphates involves forming oxygen gas and accommodating the lost of oxygen in the phosphate structure by forming condensed phosphates (e.g., pyrophosphates or metaphosphates). Thus, although  $\text{LiFePO}_4$  is a thermally stable material, this is not a rule of thumb for any phosphate or polyoxoanionic compound.

Compared to oxides, the use of polyoxoanionic structures as electrode materials supposes the addition of electrochemically inactive heavy  $\text{XO}_4$  groups, thereby lowering the theoretical specific capacity for the one electron process. Yet this decrement could be offset by a higher lithium intercalation voltage. As stated by Goodenough et al.<sup>16</sup> in polyoxoanionic structures possessing  $M\text{--}O\text{--}X$  bonds, it is possible to act on the nature of  $X$  to change the ionic-covalent character of the  $M\text{--}O$  bonding through the inductive effect of the counteranion, in order to establish a systematic mapping and tuning of transition-metal redox potentials. For instance, with the use of the phosphate polyanions  $\text{PO}_4^{3-}$ , the  $\text{Fe}^{3+}/\text{Fe}^{2+}$  and  $\text{V}^{4+}/\text{V}^{3+}$  redox couples lie at higher potentials than when in the oxide form.<sup>17</sup> The quantification of voltage shifts in polyoxoanionic compounds is a straightforward operation for first-principles calculations.<sup>18,19</sup> It is found that for a given structural type and redox couple the voltage shift is correlated to the electronegativity of the central atom of the polyhedra,  $X$  in  $\text{XO}_4$ . Particular structural factors affecting the lithium insertion voltage in phosphates have been identified utilizing a

large data set of calculated lithium insertion voltages.<sup>4</sup> Together with the nature of the redox couple, the voltage is driven by the electrostatic of the crystal lattice, the P/O ratio and the P–O bond length.

Most polyoxoanionic materials are insulating compounds with band gaps of the order of 3 eV (see, for instance, ref 19) and electronic conductivity occurs by polaron hopping. Generally speaking, the lower electronic conductivity of polyoxoanion materials leads to lower rate capabilities compared to oxides. DFT+U investigations offer the opportunity to explore the electronic conductivity in  $\text{LiFePO}_4$  by polaron hopping.<sup>20</sup> As many promising new cathode material classes such as silicates, borates, and sulfates are electrically insulating materials, polaron conduction prediction by advanced calculation methods are urgently needed to predict the rate capability of these materials.

**4.1. Olivine  $\text{LiMPO}_4$ .** Among the polyoxoanionic structures, the olivine- $\text{LiFePO}_4$  material has received most attention due to its excellent electrochemical properties. At room temperature extraction of Li ions from  $\text{LiFePO}_4$  proceeds via a biphasic process in which the final  $\text{FePO}_4$  (isostructural with heterosite) structure is obtained through minimum displacement of the ordered phosphor-olivine framework. In the  $\text{LiFePO}_4$  phase diagram an unusual eutectoid transition to the solid solution phase at about 400 °C was found experimentally<sup>21</sup> and computationally.<sup>22</sup>

Experimentally the poor electronic conductivity of olivine- $\text{LiFePO}_4$  is overcome by carbon coating techniques. This leaves ionic mobility as the limiting factor for rate capability.

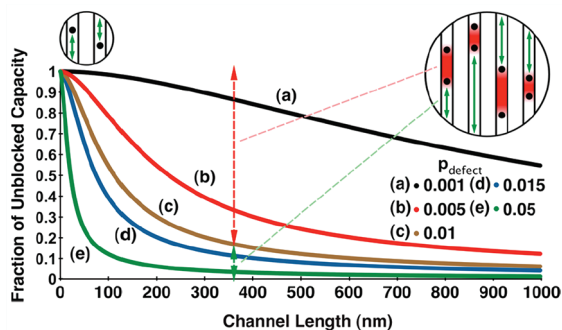


**FIGURE 6.** Expected unblocked capacity vs channel length in  $\text{LiFePO}_4$  for various defect concentrations. Reprinted with permission from 25. Copyright 2010 American Chemical Society.

DFT investigation showed that the Li hopping *between* the chains of edge sharing octahedrons (see Figure 3c) is highly unfavorable at room temperature, with activation barriers more than 1 eV.<sup>23</sup> Using nanostructured electrodes, better rate capabilities can be obtained because the distance over which Li ion must diffuse in the solid state is dramatically decreased. Simulations of  $\text{LiFePO}_4$  materials helped to elucidate the ultrafast delithiation processes of nano- $\text{LiFePO}_4$ .<sup>24</sup> The authors investigated several surface properties of olivine structure  $\text{LiFePO}_4$  and found the calculated surface energies and surface redox potentials to be very anisotropic. The two low-energy surfaces (010) and (201) dominate in the Wulff (equilibrium) crystal shape and make up almost 85% of the surface area. More interestingly in ref 24, the Li redox potential for the (0 1 0) surface is calculated to be 2.95 V, which is significantly lower than the bulk value of 3.55 V. This study reveals the importance of controlling both the size and morphology of nanoelectrode materials.

In recent years, it has been revealed that Li and Fe exchanges sites under most of the synthetic conditions and the amount of Li–Fe antisite defects can be as high as 10%. A recent first-principles study by Malik et al.<sup>25</sup> demonstrated that the Fe residing on Li sites impedes fast 1D transport along the [010] direction. Li trapped between the antisite defects cannot access fast 1D diffusion in and out of the particle, and as the particle size is increased, all Li become trapped for any finite defect concentration (Figure 6). The diffusivity in defective  $\text{LiFePO}_4$  is determined by first-principles calculation, which shows in the presence of modest defect concentrations, Li transport in nano- $\text{LiFePO}_4$  is orders of magnitude faster than in large particles.

Computational work has also been crucial in the investigation of high pressure driven transformations of olivine electrode materials. Contrary to temperature, pressure is an

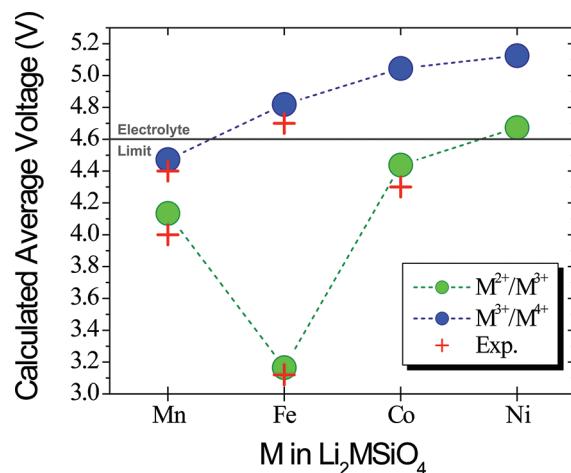


**FIGURE 7.** Prediction of lithium insertion voltages for  $\text{Li}_2\text{MSiO}_4$  compounds. Crosses indicate the experimental values. Adapted from ref 19 with permission from Elsevier.

easy parameter for DFT methods. The combination of DFT methods and experiments has led to the preparation of several novel  $\text{Li}_x\text{MXO}_4$  high pressure polymorphs compounds ( $M = \text{Mn, Fe, Co, Ni}$  and  $X = \text{P, As}$ ), crystallizing in the  $\text{Na}_2\text{CrO}_4$  and spinel structural types (refs 26 and 27, and references therein). Despite the better electronic conductivity of the high pressure materials, the low lithium mobility results in poor electrochemical performance of the high pressure forms of olivine- $\text{Li}_x\text{FePO}_4$  ( $x = 0, 1$ ) as positive electrode for lithium batteries.

**4.2. Silicates  $\text{Li}_2\text{MSiO}_4$ .** Current strategies to increase the specific energy of cathode materials pursue the development of materials displaying high specific capacities, beyond the one electron process offered by commercialized materials. The  $\text{Li}_2\text{MSiO}_4$  ( $M = \text{Fe, Mn, Co, Ni}$ ) family is attractive due to the at least theoretical possibility to reversibly deintercalate two lithium equivalents from the structure. The voltage of the redox processes  $M^{2+}/M^{3+}$  and  $M^{3+}/M^{4+}$  were predicted in 2006,<sup>19</sup> and some of these predictions were later experimentally confirmed.<sup>28,29</sup> As seen in Figure 7, in terms of lithium intercalation voltage,  $\text{Li}_2\text{MnSiO}_4$  is the best candidate for the two electron process. However, joint computational and experimental work demonstrated that the crystal structure of  $\text{Li}_2\text{MnSiO}_4$  collapses under lithium deinsertion,<sup>30</sup> forming a  $\text{MnSiO}_4$  structure built by edge-sharing  $\text{Mn}^{4+}$  octahedra. This is not surprising; in the  $\text{Li}_2\text{MSiO}_4$  structures, TM occupy tetrahedral sites and there is a strong driving force for most  $M^{3+}$  and  $M^{4+}$  ions to change the coordination upon lithium extraction and the structure of  $\text{MSiO}_4$  to transform into a more stable structure or to collapse.<sup>19,31</sup>

$\text{Li}_2\text{MSiO}_4$  compounds exhibit a rich polymorphism, adopting a large variety of crystal structures related to

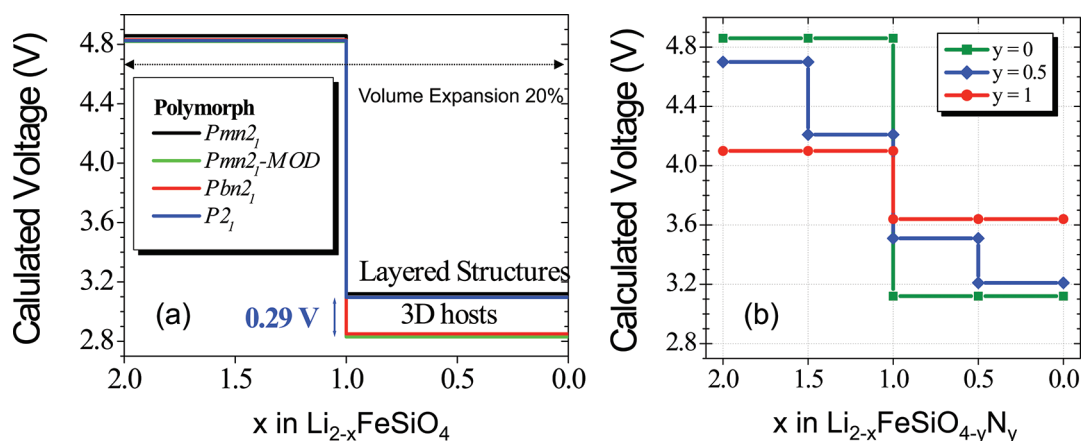


**FIGURE 8.** (a) Influence of polymorphism in the voltage composition profile of  $\text{Li}_2\text{FeSiO}_4$ . Adapted with permission from 34. Copyright 2012 American Chemical Society. (b) Calculated voltage Li composition profiles for  $\text{Li}_2\text{FeSiO}_4$  (green),  $\text{Li}_2\text{FeSi}_{3.5}\text{N}_{0.5}$  (blue), and  $\text{Li}_2\text{FeSiO}_3\text{N}$  (red). Reproduced from 35 by permission of The Royal Society of Chemistry.

$\text{Li}_3\text{PO}_4$  polymorphs but showing a different connectivity for the  $[\text{SiO}_4]$ ,  $[\text{LiO}_4]$ , and  $[\text{MO}_4]$  tetrahedral units.<sup>28,32</sup> Both experiments<sup>28,32</sup> and calculations<sup>33,34</sup> agree that the crystal structure has little impact on the general characteristics of the known polymorphs. For various  $\text{Li}_2\text{FeSiO}_4$  polymorphs, calculations predict that the deinsertion of the second Li ion occurs at a very high voltage (Figure 8a). This process is accompanied by a notorious volume expansion (20%) and the creation of holes in the O-2p band,<sup>35</sup> both factors being detrimental for the structural stability of highly delithiated phases. In addition, the calculated minimum lithium migration barriers are as large of 0.8–0.9 eV.<sup>36,37</sup> In view of the above, structural and/or compositional modifications are required to turn  $\text{Li}_2\text{MSiO}_4$  into competitive material. Compositional modifications involving the oxoanion are an interesting approach to modify the properties of  $\text{Li}_2\text{MSiO}_4$  silicates. A possible strategy is the substitution of O ions by other first row p-elements. It has been recently predicted that the electrochemical characteristics of  $\text{Li}_2\text{FeSiO}_4$  are improved in the N substituted compounds  $\text{Li}_2\text{FeSiO}_{4-y}\text{N}_y$  ( $y = 0.5, 1$ ),<sup>35</sup> as can be seen in the predicted voltage–composition profile shown in Figure 8b. The high theoretical specific capacity of  $\text{Li}_2\text{FeSiO}_4$  (330 mAh/g) could be retained in N-substituted silicates thanks to the oxidation of  $\text{N}^{3-}$  anions, which is predicted to be in a voltage range of ca. 3.5–4.2 V. In the light of the potential benefits, N substitution for O experimental work is encouraged, in particular to investigate the reversibility and overpotential of the N redox reaction. Contrary to the beneficial effect of N-substitution, it has been predicted that F substitution is detrimental for the materials performance.<sup>38</sup> Fluorine substitution is generally considered to shift the electrode materials potential to be more positive. Computational investigation of virtual materials

based on  $(\text{X}^{z+}\text{O}_{4-y}\text{F}_y)^{z+y-8}$  units<sup>39</sup> predicts that the redox potential would become more positive, but only if the F ions belong to the first coordination shell of the transition metal ion that is electrochemically active (existence of M–F bonds).

**4.3. Favorite  $\text{LiMXO}_4\text{F}$ .** As discussed above, one can expect that for the same redox couple sulfates will have higher voltages than phosphates. In  $\text{LiFeSO}_4\text{F}$ , the combining effect of sulfate groups and the F counterions in the  $[\text{FeO}_4\text{F}_2]$  octahedra raises the voltage of the  $\text{Fe}^{2+}/\text{Fe}^{3+}$  redox couple to 3.6 V, compared to 3.45 V for  $\text{LiFePO}_4$ .<sup>40</sup> Similar voltage increases have been computationally predicted for a large variety of redox-couples in favorite-like  $\text{LiMXO}_4\text{F}$  ( $\text{X} = \text{P}, \text{S}$ ) compared to the isostructural  $\text{LiMXO}_4\text{O}$  ( $\text{X} = \text{P}, \text{S}$ ).<sup>3</sup> Calculated activation energies for lithium diffusion through known favorite electrode materials support experimental results that these materials are capable of very high rates of lithium diffusion.<sup>41</sup> This eliminates the need of carbon coating or nanoparticle sizing for fast rate diffusion. While deinsertion from favorite- $\text{LiMSO}_4\text{F}$  is limited to one Li ion per TM, high throughput calculations have identified several favorite-fluorophosphates that may be capable of reversibly inserting two lithium ions per TM ions metal:  $\text{V}(\text{PO}_4)\text{F}$ ,  $\text{MoO}(\text{PO}_4)$ ,  $\text{WO}(\text{PO}_4)$ , and  $\text{NbO}(\text{PO}_4)$ .<sup>3</sup>

Many essential aspects remain to be explored for the favorite-like materials, such as the interplay between lithium ordering and the electronic configuration of the TM ions,<sup>42</sup> which likely generates the different voltage–composition profile observed for  $\text{Li}_{1-x}\text{MPO}_4\text{F}$  ( $\text{M} = \text{V}, \text{Ti}, \text{Fe}$ ). First principles calculations are also expected to lead the design of promising  $\text{LiFe}_{1-x}\text{M}_x\text{SO}_4\text{F}$  favorite-like materials.<sup>43</sup> It has been recently shown that the 5% substitution of Mn for Fe in favorite- $\text{LiFeSO}_4\text{F}$  stabilized a new material with the



triplite structure.<sup>44</sup> In this novel material, the reversible deinsertion of 0.9 Li ions occurs at 3.90 V, the highest voltage ever reported for the Fe<sup>2+</sup>/Fe<sup>3+</sup> redox couple, with a small volume change of 0.6%. Future DFT works will be needed to clarify the phase stability and electrochemical properties in relation to the crystal structure for favorite and triplite LiMXO<sub>4</sub>F materials.

## 5. Concluding Remarks

In this Account, we have illustrated how first-principles computation can accelerate the search for energy storage electrode materials for lithium ion batteries. New electrode materials exhibiting high energy, high power, better safety and longer cycle life must be developed to meet the increasing demand of energy storage, particularly in transportation applications such as plug-in HEV. We have demonstrated the achievements toward predicting relevant properties (including voltage, structure stability, electronic property, etc.) of electrode materials using DFT based first-principles methods. In summary, these capabilities establish first-principles computation as an invaluable tool in designing new electrode materials for lithium ion batteries.<sup>45</sup> However, despite these capabilities, it is important to recognize that many challenges still need to be resolved; predicting new mechanisms (other than intercalation), new properties of nanoscale materials, and atomistic understanding of the surface and interphase remain as the challenges to first-principles computation. The implication of computational materials design goes far beyond the field of lithium ion battery materials. What we will see in the near future is a paradigm shift of how advanced materials discovery and deployment are done. Computational tools will be critically important to enable real-world materials development, optimization or minimization of traditional experimental testing, and prediction of materials performance under diverse conditions.

M.E.A.D. acknowledges financial support from Spanish Ministry of Science (MAT2007-62929, CSD2007-00045, and S2009/PPQ-1551). Y.S.M. expresses her gratitude to the financial support from the U.S. Department of Energy, Office of Basic Energy Sciences under Award Number DE-SC-002357. The authors thank Ms. Bo Xu for the help on constructing the figures.

## BIOGRAPHICAL INFORMATION

**Y. S. Meng** is an assistant professor at the Department of Nano-Engineering, University of California San Diego and she is the leader of the Laboratory for Energy Storage and Conversion (LESC), which focuses on designing and developing new nanostructured materials for batteries and supercapacitors.

**M. E. Arroyo-de Dompablo** obtained her Ph.D. in Chemistry from the Universidad Complutense de Madrid, where she is currently Professor of Inorganic Chemistry. Her research area is the fundamental properties of Li-ion intercalation materials, in particular their structural transformations under nonequilibrium (high pressure and/or high temperature) conditions.

## FOOTNOTES

\*E-mail: shirleymeng@ucsd.edu (Y.S.M.); e.arroyo@quim.ucm.es (M.E.A.D.). The authors declare no competing financial interest.

## REFERENCES

- Meng, Y. S.; Arroyo-de Dompablo, M. E. First principles computational materials design for energy storage materials in lithium ion batteries. *Energy Environ. Sci.* **2009**, *2*, 589–609.
- Jain, A.; Hautier, G.; Moore, C. J.; Ong, S. P.; Fischer, C. C.; Mueller, T.; Persson, K. A.; Ceder, G. A high-throughput infrastructure for density functional theory calculations. *Comput. Mater. Sci.* **2011**, *50*, 2295–2310.
- Mueller, T.; Hautier, G.; Jain, A.; Ceder, G. Evaluation of Favorite-Structured Cathode Materials for Lithium-Ion Batteries Using High-Throughput Computing. *Chem. Mater.* **2011**, *23*, 3854–3862.
- Hautier, G.; Jain, A.; Ong, S. P.; Kang, B.; Moore, C.; Doe, R.; Ceder, G. Phosphates as Lithium-Ion Battery Cathodes: An Evaluation Based on High-Throughput ab Initio Calculations. *Chem. Mater.* **2011**, *23*, 3495–3508.
- Van der Ven, A.; Ceder, G. In *Lithium Batteries*; Nazri, G.-A., Pistoia, G., Eds.; Kluwer Academic Publishers: New York, 2004; pp 42–84.
- Kang, K.; Ceder, G. Factors that affect Li mobility in layered lithium transition metal oxides. *Phys. Rev. B* **2006**, *74*, 094105-1–094105-7.
- Kang, K. S.; Meng, Y. S.; Breger, J.; Grey, C. P.; Ceder, G. Electrodes with high power and high capacity for rechargeable lithium batteries. *Science* **2006**, *311*, 977–980.
- Breger, J.; Meng, Y. S.; Hinuma, Y.; Kumar, S.; Kang, K.; Shao-Horn, Y.; Ceder, G.; Grey, C. P. Effect of high voltage on the structure and electrochemistry of LiNi<sub>0.5</sub>Mn<sub>0.5</sub>O<sub>2</sub>: A joint experimental and theoretical study. *Chem. Mater.* **2006**, *18*, 4768–4781.
- Thackeray, M. M.; Kang, S. H.; Johnson, C. S.; Vaughey, J. T.; Benedek, R.; Hackney, S. A. Li<sub>2</sub>MnO<sub>3</sub>-stabilized LiMO<sub>2</sub> (M = Mn, Ni, Co) electrodes for lithium-ion batteries. *J. Mater. Chem.* **2007**, *17*, 3112–3125.
- Xu, B.; Fell, C. R.; Chi, M. F.; Meng, Y. S. Identifying surface structural changes in layered Li-excess nickel manganese oxides in high voltage lithium ion batteries: A joint experimental and theoretical study. *Energy Environ. Sci.* **2011**, *4*, 2223–2233.
- Ohzuku, T.; Kitagawa, M.; Hirai, T. Electrochemistry of Manganese Dioxide in Lithium Nonaqueous Cell III. X-Ray Diffractonal Study on the Reduction of Spinel-Related Manganese Dioxide. *J. Electrochem. Soc.* **1990**, *137*, 769–775.
- Xu, B.; Meng, Y. S. Factors affecting Li mobility in spinel LiMn<sub>2</sub>O<sub>4</sub>: A first-principles study by GGA and GGA+U methods. *J. Power Sources* **2010**, *195*, 4971–4976.
- Yang, M. C.; Xu, B.; Cheng, J. H.; Pan, C. J.; Hwang, B. J.; Meng, Y. S. Electronic, Structural, and Electrochemical Properties of LiNi<sub>1-x</sub>Cu<sub>y</sub>Mn<sub>2-x-y</sub>O<sub>4</sub> (0 < x < 0.5, 0 < y < 0.5) High-Voltage Spinel Materials. *Chem. Mater.* **2011**, *23*, 2832–2841.
- Biskup, N.; Martinez, J. L.; de Dompablo, M.; Diaz-Carrasco, P.; Morales, J. Relation between the magnetic properties and the crystal and electronic structures of manganese spinels LiNi<sub>0.5</sub>Mn<sub>1.5</sub>O<sub>4</sub> and LiCu<sub>0.5</sub>Mn<sub>1.5</sub>O<sub>4-δ</sub> (0 < δ < 0.125). *J. Appl. Phys.* **2006**, *100*, 093908.
- Arroyo de Dompablo, M. E.; Morales, J. A first-principles investigation of the role played by oxygen deficiency in the electrochemical properties of LiCu<sub>0.5</sub>Mn<sub>1.5</sub>O<sub>4-δ</sub> spinels. *J. Electrochem. Soc.* **2006**, *153*, A2098–A2102.
- Padhi, A. K.; Manivannan, V.; Goodenough, J. B. Tuning the position of the redox couples in materials with NASICON structure by anionic substitution. *J. Electrochem. Soc.* **1998**, *145*, 1518–1520.
- Masquelier, C.; Patoux, S.; Wurm, C.; Morcrette, M. In *Lithium Batteries*; Nazri, G.-A., Pistoia, G., Eds.; Kluwer Academic Publishers: New York, 2004; pp 445–477.
- Arroyo-de Dompablo, M. E.; Rozier, P.; Morcrette, M.; Tarascon, J. M. Electrochemical data transferability within Li<sub>2</sub>VOXO<sub>4</sub> (X = Si, Ge<sub>0.5</sub>Si<sub>0.5</sub>, Ge, Si<sub>0.5</sub>As<sub>0.5</sub>, Si<sub>0.5</sub>P<sub>0.5</sub>, As, P) polyoxyanionic compounds. *Chem. Mater.* **2007**, *19*, 2411–2422.
- Arroyo-de Dompablo, M. E.; Armand, M.; Tarascon, J. M.; Amador, U. On-demand design of polyoxianionic cathode materials based on electronegativity correlations: An exploration of the Li<sub>2</sub>MSiO<sub>4</sub> system (M = Fe, Mn, Co, Ni). *Electrochem. Commun.* **2006**, *8*, 1292–1298.
- Maxisch, T.; Zhou, F.; Ceder, G. Ab initio study of the migration of small polarons in olivine Li<sub>2</sub>FePO<sub>4</sub> and their association with lithium ions and vacancies. *Phys. Rev. B* **2006**, *73*, 104301-1–104301-7.
- Delacourt, C.; Poizot, P.; Tarascon, J.-M.; Masquelier, C. The existence of a temperature-driven solid solution in Li<sub>x</sub>FePO<sub>4</sub> for 0 < x < 1. *Nat. Mater.* **2005**, *4*, 254–260.

- 22 Zhou, F.; Maxisch, T.; Ceder, G. Configurational electronic entropy and the phase diagram of mixed-valence oxides: The case of  $\text{Li}_x\text{FePO}_4$ . *Phys. Rev. Lett.* **2006**, *97*, 155704-1–155704-9.
- 23 Morgan, D.; Van der Ven, A.; Ceder, G. Li conductivity in  $\text{Li}_x\text{MPO}_4$  ( $M = \text{Mn, Fe, Co, Ni}$ ) olivine materials. *Electrochem. Solid-State Lett.* **2004**, *7*, A30–A32.
- 24 Wang, L.; Zhou, F.; Meng, Y. S.; Ceder, G. First-principles study of surface properties of  $\text{LiFePO}_4$ : Surface energy, structure, Wulff shape, and surface redox potential. *Phys. Rev. B* **2007**, *76*, 16435-1–16435-11.
- 25 Malik, R.; Burch, D.; Bazant, M.; Ceder, G. Particle Size Dependence of the Ionic Diffusivity. *Nanoletters* **2010**, *10*, 4123–4127.
- 26 Arroyo y de Dompablo, M. E.; Biskup, N.; Gallardo-Amores, J. M.; Moran, E.; Ehrenberg, H.; Amador, U. Gaining Insights into the Energetics of  $\text{FePO}_4$  Polymorphs. *Chem. Mater.* **2010**, *22*, 994–1001.
- 27 Amador, U.; Gallardo-Amores, J. M.; Heymann, G.; Huppertz, H.; Moran, E.; Arroyo-de Dompablo, M. E. High pressure polymorphs of  $\text{LiCoPO}_4$  and  $\text{LiCoAsO}_4$ . *Solid State Sci.* **2008**, *11*, 343–348.
- 28 Lyness, C.; Delobel, B.; Armstrong, A. R.; Bruce, P. G. The lithium intercalation compound  $\text{Li}_2\text{CoSiO}_4$  and its behaviour as a positive electrode for lithium batteries. *Chem. Commun.* **2007**, 4890–4892.
- 29 Muraliganth, T.; Stroukoff, K. R.; Manthiram, A. Microwave-Solvothermal Synthesis of Nanostructured  $\text{Li}_2\text{MSiO}_4/\text{C}$  ( $M = \text{Mn}$  and  $\text{Fe}$ ) Cathodes for Lithium-Ion Batteries. *Chem. Mater.* **2010**, *22*, 5754–5761.
- 30 Kokalj, A.; Dominko, R.; Mali, G.; Meden, A.; Gaberscek, M.; Jamnik, J. Beyond one-electron reaction in Li cathode materials: Designing  $\text{Li}_2\text{Mn}_x\text{Fe}_{1-x}\text{SiO}_4$ . *Chem. Mater.* **2007**, *19*, 3633–3640.
- 31 Arroyo-de Dompablo, M. E.; Gallardo-Amores, J. M.; Garcia-Martinez, J.; Moran, E.; Tarascon, J. M.; Armand, M. Is it possible to prepare olivine-type  $\text{LiFeSiO}_4$ ? A joint computational and experimental investigation. *Solid State Ionics* **2008**, *179*, 1758–1762.
- 32 Sirisopanaporn, C.; Masquelier, C.; Bruce, P. G.; Armstrong, A. R.; Dominko, R. Dependence of  $\text{Li}_2\text{FeSiO}_4$  Electrochemistry on Structure. *J. Am. Chem. Soc.* **2011**, *133*, 1263–1265.
- 33 Arroyo-de Dompablo, M. E.; Dominko, R.; Gallardo-Amores, J. M.; Dupont, L.; Mali, G.; Ehrenberg, H.; Jamnik, J.; Moran, E. On the energetic stability and electrochemistry of  $\text{Li}_2\text{MnSiO}_4$  polymorphs. *Chem. Mater.* **2008**, *20*, 5574–5584.
- 34 Saracibar, A.; Van de Ven, A.; Arroyo-de Dompablo, M. E. Crystal structure, energetics and electrochemistry of  $\text{Li}_2\text{FeSiO}_4$  polymorphs from first principles calculations. *Chem. Mater.* **2012**, *24*, 495–503.
- 35 Armand, M.; Arroyo-de Dompablo, M. E. Benefits of N for O substitution in polyoxoanionic electrode materials: a first principles investigation of the electrochemical properties of  $\text{Li}_2\text{FeSiO}_{4-y}\text{N}_y$  ( $y = 0, 0.5, 1$ ). *J. Mater. Chem.* **2011**, *21*, 10026–10034.
- 36 Livat, A.; Thomas, J. O. Li-ion migration in  $\text{Li}_2\text{FeSiO}_4$ -related cathode materials: A DFT study. *Solid State Ionics* **2011**, *192*, 58–64.
- 37 Armstrong, A. R.; Kuganathan, N.; Islam, M. S.; Bruce, P. G. Structure and Lithium Transport Pathways in  $\text{Li}_2\text{FeSiO}_4$  Cathodes for Lithium Batteries. *J. Am. Chem. Soc.* **2011**, *133*, 13031–13035.
- 38 Armand, M.; Tarascon, J. M.; Arroyo-de Dompablo, M. E. Comparative computational investigation of N and F substituted polyoxoanionic compounds: The case of  $\text{Li}_2\text{FeSiO}_4$  electrode material. *Electrochem. Commun.* **2011**, *113*, 1047–1050.
- 39 Arroyo y de Dompablo, M. E.; Amador, U.; Tarascon, J. M. A computational investigation on fluorinated-polyanionic compounds as positive electrode for lithium batteries. *J. Power Sources* **2007**, *174*, 1251–1257.
- 40 Recham, N.; Chotard, J. N.; Dupont, L.; Delacourt, C.; Walker, W.; Armand, M.; Tarascon, J. M. A 3.6 V lithium-based fluorosulphate insertion positive electrode for lithium-ion batteries. *Nat. Mater.* **2010**, *9*, 68–74.
- 41 Tripathi, R.; Gardiner, G. R.; Islam, M. S.; Nazar, L. F. Alkali-ion Conduction Paths in  $\text{LiFeSO}_4\text{F}$  and  $\text{NaFeSO}_4\text{F}$  Tavorite-Type Cathode Materials. *Chem. Mater.* **2011**, *23*, 2278–2284.
- 42 Arroyo y de Dompablo, M. E.; Marianetti, C.; Van der Ven, A.; Ceder, G. Jahn-Teller mediated ordering in layered  $\text{Li}_i\text{MO}_2$  compounds. *Phys. Rev. B* **2001**, *6314*, 144107.
- 43 Frayret, C.; Villesuzanne, A.; Spaldin, N.; Bousquet, E.; Chotard, J. N.; Recham, N.; Tarascon, J. M.  $\text{LiMSO}_4\text{F}$  ( $M = \text{Fe, Co}$  and  $\text{Ni}$ ): promising new positive electrode materials through the DFT microscope. *Phys. Chem. Chem. Phys.* **2010**, *12*, 15512–15522.
- 44 Barpanda, P.; Ati, M.; Melot, B. C.; Rousse, G.; Chotard, J. N.; Doublet, M. L.; Sougrati, M. T.; Corr, S. A.; Jumas, J. C.; Tarascon, J. M. A 3.90 V iron-based fluorosulphate material for lithium-ion batteries crystallizing in the triplite structure. *Nat. Mater.* **2011**, 772–779.
- 45 <http://www.materialsproject.org/>.